Regioselective and Anisotropic Multi-Patching of Small Microparticles via a Polymer Brush-Assisted Microcontact Printing (µCP)

Martin Reifarth,#[ab]* Marcel Sperling,#[b] Richard Grobe,[a] Pinar Akarsu,[ab] Maurice Schmette,[ab] Steffen Tank,[c] Katja M. Arndt,[c] Salvatore Chiantia,[d] Matthias Hartlieb,[ab] Alexander Böker[ab]*

a Institute of Chemistry, University of Potsdam, Karl-Liebknecht-Straße 24-25, 14476, Potsdam, Germany

b Fraunhofer Institute for Applied Polymer Research (IAP), Geiselbergstraße 69, 14476, Potsdam, Germany

c Molecular Biotechnology, Institute of Biochemistry and Biology, University of Potsdam, Karl-Liebknecht-Straße 24-25, 14476, Potsdam, Germany

d Physical Biochemistry, Institute of Biochemistry and Biology, University of Potsdam, Karl-Liebknecht-Straße 24-25, 14476, Potsdam, Germany

#Both authors contributed equally to this work.

*Corresponding authors: martin.reifarth@uni-potsdam.de, alexander.boeker@iap.fraunhofer.de

Abstract:

We developed a method for fabricating anisotropic monodisperse silicon dioxide (SiO_2) patchy microspheres. The protocol utilizes a modified microcontact printing (µCP) technique, employing a polydimethylsiloxane (PDMS) elastomer with a regularly grooved surface topography as a stamp. The stamp's microscale channels create a confined environment for the SiO_2 microspheres, as they match the particle dimensions (~4 µm). Our solid-phase µCP routine allows for the transfer of functional trialkoxysilanes from the elastomer stamp to the particles exclusively at their contact faces. By applying a second stamp to the exposed side of the particles, a fourth patch with different chemical information

is added. This fabrication process, compatible with various follow-up chemistries, adds patches with adjustable characteristics. The method is suitable to fabricate particles possessing a C_{4v} and C_{2v} symmetry. Importantly, the protocol is easily adaptable to other particle dimensions and surface chemistries, indicating significant potential in the field of anisotropically functionalized spherical colloidal particles.

Introduction:

The unique asymmetric characteristics of patchy particles, i.e. nano- or microscale materials with distinct surface domains, have intrigued material scientists for years.[1,2] Their inherent asymmetry enables patchy particles to spontaneously assemble into larger structures with specific geometries, making them promising candidates for the bottom-up creation of complex materials.[3–6] Patches can be classified as either enthalpic or entropic,[6] referring to chemical surface alterations or topological variations like protrusions or dimples, respectively.[6]

Despite the outlined potential in material science,[7–9] there are relatively few publications demonstrating the self-assembly of complex particle architectures experimentally.[10] A significant challenge is the manufacturing of suitable patchy materials in a controllable and scalable fashion, particularly when aiming at a high asymmetry in patch distribution along with a preeminent functionality of the patch material. Fabrication strategies of patchy particles involve syntheses in bulk as well as interfacial modification protocols.[4] Bulk syntheses start from selected precursors yielding well-defined particles, e.g. via the seeded-growth mechanism starting from spherical particles, which are subjected to heterogenous nucleation at the particle surface.[10–15] Such reactions yield particle clusters that can be considered entropically patched particles, whose morphologies result from the minimization of surface energies of the initial and the superficially grown particles.[10–15] Another fabrication strategy relies on functional block-copolymers that may undergo a phase-separation process driven by the thermodynamics of macromolecular block-copolymer architectures in an aqueous environment.[16,17] Furthermore, controlled colloidal fusion processes can be applied for the

preparation of patchy particles, which exploits the coordination dynamics of particles to well-defined clusters and the subsequent chemical fixation of these aggregates by embedding them into a polymeric matrix.[12,18,19] Even though these techniques yield well-defined particles in a scalable fashion, patches are often entropic in nature lacking chemical functionality.

Alternatively, the surface post-functionalization of isotropic particles at an interface can be employed. This strategy is more versatile, as it is applicable to many different starting materials. A very prominent example is the formation of *Janus*-type particles at the interface of Pickering emulsions.[20–22] In contrast, dry preparation techniques start from particles that are deposited as a monolayer on a surface, and, next, functionalized at the exposed surface. Glancing-angle deposition (GLAD), as an example, uses metal vapor for particle functionalization. This process yields particles with uniform patches, even with complex patch geometries, but is applicable only to metals as patch materials.[23–25] Microcontact printing (μCP) represents a more versatile fabrication method towards highly functional patchy particles.[26] Here, a particle monolayer is modified using a chemical modification agent, referred to as the μCP ink, from an elastomeric stamp by physical contact,[27] introducing chemical functionality on the particle caps.[28–31] Recently, we demonstrated a polymer brush-supported μCP protocol[32,33] can be used for the asymmetric functionalization of silicon dioxide (SiO_2) microspheres with polymer patches.[34]

Despite this versatility from a materials perspective, most described methods are geometrically restricted. Accordingly, Pickering emulsions merely enabling synthesis of mono-patchy particles. Also, the method of μCP comes along with these geometrical restrictions, as usually only Janus-[28–30] or sandwich-type bipatchy colloids[31] can be fabricated. A recent study, however, projected the tremendous capacity of three- to four-patched particles for self-assembly.[35] While recent work demonstrated the fabrication of highly anisotropic multi-patchy particles via bulk-electrosynthesis, this protocol was limited to metal patches on particles in the millimeter size range.[36]

We were therefore intrigued by the possibility of establishing a fabrication technique of anisotropic (SiO_2) patchy microspheres – in the low μm regime – possessing up to four patches at their equatorial

side using a µCP protocol. To warrant a suitable binding affinity of the patch material to the particles combined with a high chemical functionality, alkoxysilanes were employed.[37] Their locally precise attachment is thereby achieved using a polymer-assisted microcontact printing routine.[32–34,38] Using groove stamps with pre-determined dimensions forming a confined environment for the particles, we are able to print up to four enthalpic patches on the particle faces with a defined surface chemistry, which offers chemically orthogonal binding sides holding tremendous potential for downstream applications.

Results and Discussion:

The starting material for fabricating our patchy particles were silicon dioxide microspheres with a nominal diameter of 4.08 µm. These particles represent commercially available colloidal particles combining a versatile functionalization capability with a sufficient chemical stability. Since SiO_2 particles are robust towards the influence of, *e.g.* mild acids and bases as well as most organic solvents, they can be subjected to a variety of (chemical) manipulation protocols without loss of integrity. All further functionalization makes use of the introduction of reactive silicic acid derivatives, being well-known functionalization agents for silicon oxide surfaces,[37] namely (3-aminopropyl)triethoxysilane (APTES) used in this study. The printing process is based on the utilization of a structured stamp possessing channels with dimensions matching the particles' sizes, as shown in **Figure *1*** (the preparation of the stamp is illustrated in Figure S1). For printing, the particles are lined up inside the channels, localizing them in between the channel walls. An additional stamp applied to the exposed side of the particle can add a supplementary patch, which may consist of a material that differs from the residual patches.

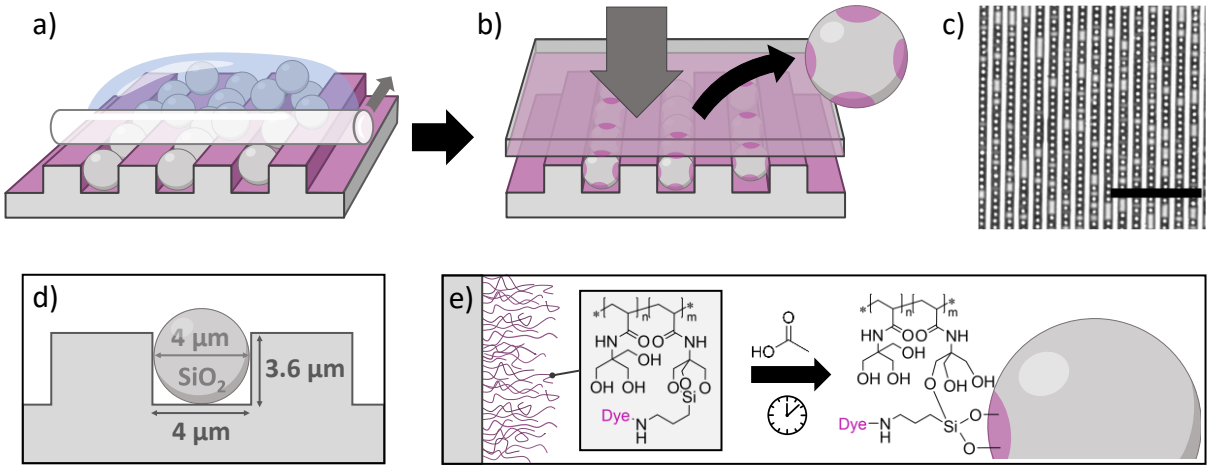

Figure 1: Schematic representation of the overall protocol. a) For µCP, particles are deposited in a PDMS stamp and aligned inside the grooves via shearing using a glass rod. b) Printing occurs via a second flat stamp from the exposed side and yields particles possessing four patches in an equatorial position at the particle body. c) Transmission light microscopy image of a stamp with deposited particles showing the alignment (scale bar = 50 µm). d) The first stamp possesses grooves matching the particle diameter and leaving the caps exposed. Printing occurs under a defined mild pressure on the particle sides that directly face the stamp interface. e) The ink (labelled APTES) is therefore transferred in a locally and temporarily defined fashion from PTrisAAm brushes on the stamp. APTES is covalently, though reversibly, bound to PTrisAAm, and transferred to the particle interface under the presence of acetic acid vapour as catalyst.

There are two major requirements for the process: The printing process must be (i) locally and (ii) temporarally precise. The local precision of the printing process (i) is required to add locally defined patches to the particles. The capillary activity of the particle surface thereby undermines a precise transfer by promoting the diffusive spread of the ink, leading to smearing, which would reduce the local accuracy of the patches and thus adversely affect the directional information of the particles. The temporal precision (ii) of the printing process refers to the controllability of the timing of ink transfer. The deposition of the particles inside the grooves represents the crucial step of the process. As the particles slide into the grooves during the alignment process, prompt functionalization kinetics could cause an ink transfer to the particle surfaces when they are still in motion. For precise patterning, however, ink transfer must occur precisely when the particles are in a steady position.

To fulfil these requirements, we applied a modified microcontact printing (µCP) routine optimized for the controlled transfer of APTES.[32–34] Accordingly, we use PDMS equipped with polymer brushes via reversible addition-fragmentation chain-transfer (RAFT) polymerization.[34] The polymer, poly{*N*-[tris(hydroxymethyl)methyl] acrylamide} (PTrisAAm), possesses three hydroxy groups per monomeric

unit. With these features, APTES can be bound to the polymer matrix as depicted in **Figure 1e** and outlined in section 2.2 of the supplementary information. In this binding mode, the APTES ink is immobilized in a covalent, though reversible fashion. Possessing an increased affinity to an oxidic substrate surface, where it can bind irreversibly, the ink molecules are transferred from the polymer matrix to the surface of the substrate, when stamp and substrate are brought into physical contact. These features enable a spatially controllable transfer, ensuring a locally defined printing. As the printing reaction, moreover, requires the presence of a catalytical amount of an acid, temporal control can be achieved by timing of acid addition to the reaction. The underlying chemistry including the rationales of the preparation of the functional stamps is illustrated in more detail in **Figure S1** and **S2**.

The first step of the protocol ensures an efficient placement of the particles inside the stamp channels. This is facilitated *via* a shear-induced assembly process,[39] during which a defined volume of a suspension of the pristine particles is dropped on the PDMS stamp, and a glass rod oriented orthogonally to the stamp grooves is pulled with a constant velocity over the stamp (**Figure 1a**). A transmission light microscopy image (**Figure 1c**) reveals that the particles are localized inside the grooves with a decent surface density, if the particles are added as a 40 mg mL^{-1} suspension in isopropanol. The optimization of this process is documented in the supplementary information of this article (**Figure S3 – S6**, and **Table S1**). Given the fact that the printing relies on the mechanical contacting of a microscale particle in a confined environment, the stamps must be homogeneously thick and comparably smooth, as even small inhomogeneities in the stamp surface can easily result in distortions in the scale of one or more particle diameters. To fulfil these experimental requirements, an optimized preparation protocol was applied as illustrated in section 3 in the supplementary information of this article.

Printing is then initiated by exposing the particle-loaded stamp to catalytical concentrations of water and acetic acid via vapour exposure. To ensure that the particles are pinched into the stamp elastomer in such a way that the particles contact each of the channel walls, a defined printing force (1 N on a 0.7 cm^2 stamp area referring to 14.3 kPa, controlled by a custom-built printing device as discussed in the supporting information of the article) is applied by pressing the stamp against a smooth surface such as a silicon wafer. Subsequently to the ink transfer process, the particles are released from the stamp for microscopy analysis. For particle release, the stamp is treated via sonication while being placed in an Eppendorf tube filled with ethanol. Here, the solvent choice is crucial to avoid hydrolysis of the inked brushes during the particle release process. For particle visualization, a labelling strategy using the amino-susceptible Alexa 555 *N*-hydroxysuccinic amide (NHS) ester or fluorescein isothiocyanate (FITC) was employed. These fluorescent labels bind specifically to the patch area, while unspecific adsorption is prevented due to the anionic nature of the dyes (which is repelled by the negatively charged SiO_2 surface).

Figure 2a and **b** show an overview image of several released particles that have been printed with three patches. A zoom in view (**Figure 2c-f**) clearly reveals the presence of numerous particles with three well-*separable* patches, which are localized in equatorial position at the particles. is to be noted that not necessarily all patches are observed, as it is likely that particles rotate or are not always oriented in the right direction with respect to the focal plane.

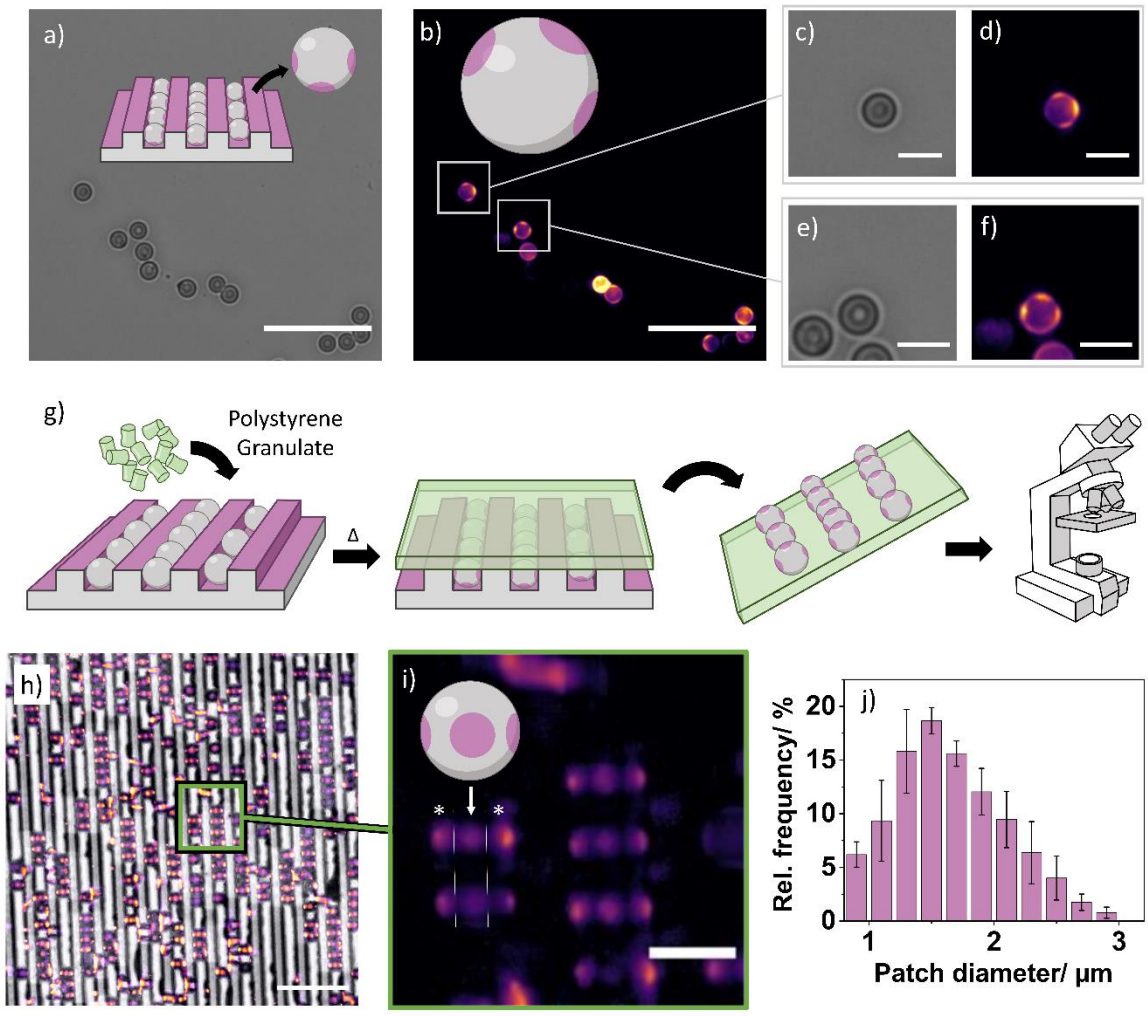

Figure 2: µCP process for the introduction of three patches with equal characteristics. a) Schematic representation of the particles released from the stamp. a), c), e) Transmission light and b), d), f) fluorescence images of released particles labelled with Alexa-555. a), b) Overview images. c) -f): Zoom-in views. g) Schematic representation of the particle preparation for direct patch observation. For this purpose, the particles are immobilized in a polystyrene (PS) film, allowing for the observation of particles directly facing the microscope objective. h) Merged light transmission (grey) and fluorescence (magenta) image of the immobilized particles. The arrow indicates the patches with direct orientation to the objective. The asterisks (*) indicate the signals corresponding to the patches with perpendicular orientation. i) Zoom-in view of the fluorescence signals of h). j) Statistical evaluation of the patch diameters with direct orientation to the microscope objective as indicated by the white arrow in i). The scale bars: a), b), h) 25 µm, c) - f), i) 5 µm.

To facilitate a more profound and quantitative evaluation of the patches, the particles are embedded into a polystyrene film while being localized in the stamp grooves as schematically depicted in **Figure 2g**. For this purpose, polystyrene (PS) granules are molten, and the particle-loaded stamp is smoothly pressed against the polymer melt. Subsequent cooling of the polystyrene melt enables to peel off the PS film, whereby the embedded particles are extracted to facilitate fluorescence microscopy analysis (**Figure 2g**). Due to the defined orientation of the particles, the patch profile can be evaluated quantitatively. **Figure 2**h shows a merged overview image (transmission image in grey and the

fluorescent signals in magenta) of the PS film with the embedded particles. The representation clearly reveals a correlation of the location of the fluorescent patch signals and the particle body, where a set of three signals is found on most particle surfaces. A zoom-in view (**Figure 2i)** provides a more profound insight into the fluorescence pattern. Accordingly, the middle signal (indicated by an arrow) corresponds to the patch that has been added from the bottom of the channel. Due to their frontal observation with respect to the microscope objective, these signals can be sized directly, whereas the periphery fluorescence (indicated by an asterisk) are axial projections of the signals with a perpendicular orientation to the observation plane (which had been transferred from the sides of the grooves). For statistical evaluation, the side signals, whose dimensions cannot directly be measured, were manually removed, and the remaining signals corresponding to the patches transferred from the channel bottom, were analyzed. Evaluation of these signals revealed patch diameters with an average of about ~ 1.5 µm with narrow patch distribution (**Figure 2**j; further details of the data analysis are shown in **Figure S7**), which confirms that the method is suitable to obtain defined patches at a low µm range. To underline the necessity of covalent ink attachment, control experiments with non-covalently inked stamps were performed (**Figure S8** and the thus obtained patches that appeared smeared and ill-defined.

After having demonstrated the transfer of three patches from the channel walls, we aimed to introduce an additional patch at the exposed side of the particle using an inked flat stamp from the top (**Figure 3a**). **Figure 3b** shows an overview image of particles still lined up in the stamp channels, after they have been subjected to printing with the top stamp (here, a pre-labelling strategy with Alexa-555 was followed). A magnified view reveals precise patches and a high number of particles remaining in the grooves. Analysis of the patch diameters clearly show that a fourth (top) patch is introduced successfully and precisely, with an average diameter of ~ 1. 5 µm. The patch size distribution is slightly larger when compared to the evaluation of bottom patch (detailed analysis in **Figure S9**).

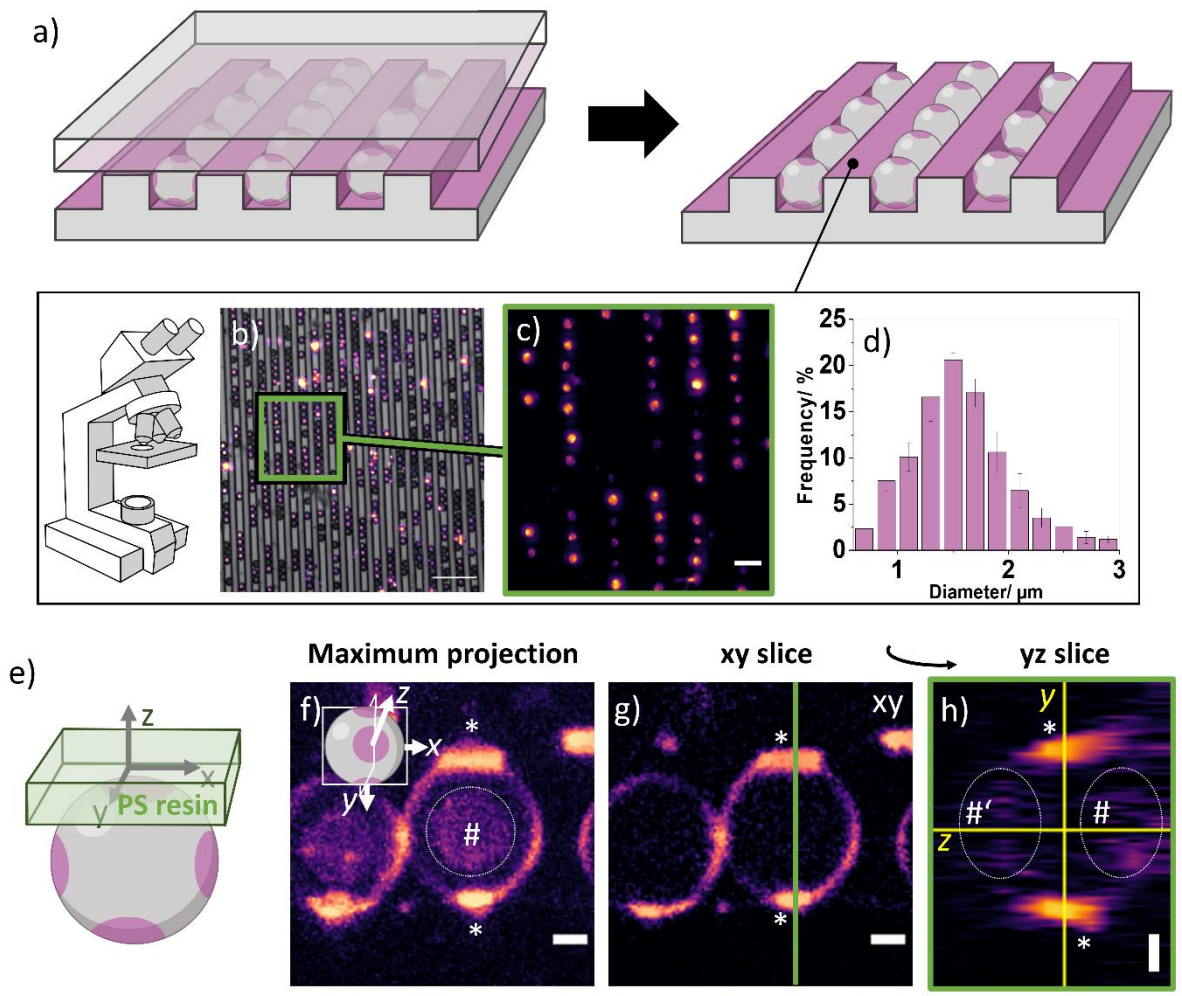

Figure 1: Fabrication of particles possessing four patches at the equatorial positions of the particles. a) Schematic overview. b) Merged light transmission and widefield fluorescence microscopy images of particles, which had been stamped from the top. c) Magnified view of the fluorescent channel of b) (highlighted area). d) Statistical analysis of the patch diameters. The histogram shows mean values and standard deviations of a triplicate of images determined at different positions of the stamp. e) Schematic representation of a particle possessing four patches, which is embedded in a PS matrix. f)-h) CLSM image of particles labelled with Alexa-555. f) Maximum projection of an axial stack of images (axes are labelled as indicated in the sketch). g) An xy plane of the particles that is recorded at the axial centre of the particle. h) An yz slice of the particle extracted at the lateral coordinates corresponding to the green line in g). In f) – h), characteristic fluorescent signals are highlighted: The signals marked with an asterisk (*) are indicative for the patches added from the sides of the stamp, whereas the encircled signals highlight the patches added from top and bottom (highlighted with a hash #). Scale bars: b) 25 µm, c) 5 µm, f)-i) 1 µm (lateral direction).

In order to obtain an insight into the three-dimensional morphology of the particles, confocal laser scanning microscopy (CLSM) was employed. For this purpose, the particles, possessing four patches, were removed from the groove stamp by embedding them in a polystyrene film as previously discussed. **Figure *1*Figure 3**e shows a schematic representation of the particles embedded into the PS resin. A projection of an axial stack of images recorded by CLSM (**Figure 3**f) shows three signals. The

signals highlighted with an asterisk (*) are indicative for the patches added from the stamp walls. Vertically oriented with respect to the focal plane of the objective, their fluorescent signals correspond to the cumulative emission of fluorophores over the axial stack, which lets these patches appear rather bright. The fluorescent signal highlighted with a hash (#) can be assigned to the patches added from top or from bottom, which are facing the objective focal plane directly. Being distributed in the lateral plane, these fluorophore signals appear less bright. **Figure 3**g shows a representative confocal slice of the particles at the axial centre of the particle. An orthogonal view at the axial coordinates as indicated by the green line in **Figure 3**g is depicted in **Figure 3**h. The yz projection of the image reveals four signals as highlighted with asterisk and hash, respectively. **Figure 3**h, thus, clearly shows the occurrence of patchy particles with four patches. These patches are also observable in the supplemental **Video V1**, where a three-dimensional reconstruction of the image stack, rotating around a lateral axis, is shown. The particles shown in Figure 3 possess an overall C_{4v} symmetry with four uniform patches, which are all placed at the equatorial side of the particles. Particles that were deposited in the stamp could also be released using ultrasonication. Patched particles were thus obtained in suspension. To remove the particles that have not been labelled from patched particles, we conducted fluorescence-activated cell sorting (FACS, Figures S10, S11). The particles separated by FACS clearly show a fluorescence signal. However, it was not possible to directly correlate the intensity of the fluorescent signals to the number of transferred patches.

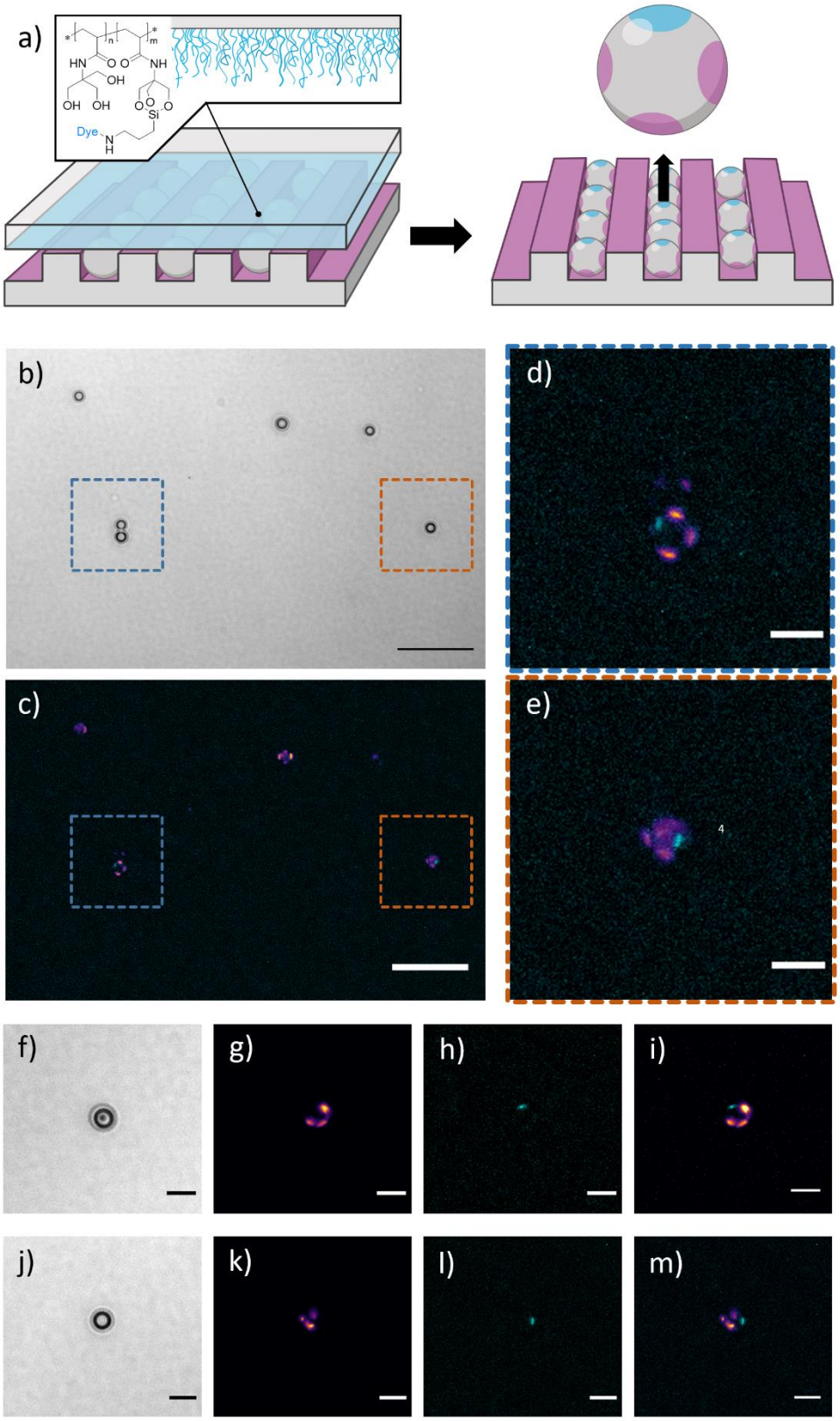

Figure 2: Microscopy images of particles possessing four different patches. a) Schematic representation. b), c) Overview, d), e) zoom-in views. f)-i) as well as j)-m) show representative particles. b), f), j) Light transmission, d)-e), g)-i), k)-m) fluorescence images. Fluorescent signals transferred from g), k) the channel walls, as well as h), l) from the top stamp. d), e), i), m) Fluorescent signals from all contacting faces in a merged view. Scale bars: b), c) 25 µm, d)-m) 5 µm.

Pre-functionalizing the APTES ink before printing allows to introduce two different, possibly orthogonal materials, for functionalization. This feature enables to engineer particles that possess a high degree of anisotropy as schematically depicted in **Figure 4**a, retaining a symmetry that can be described by the C_{2v} point group. These particles could have tremendous impact in, e.g. self-assembly, where the two chemically different surface functions could facilitate a hierarchical assembly of the patchy particles. We were therefore motivated to implement these structures experimentally. For this purpose, we selected two orthogonal fluorescent labels for functionalization and successfully produced hetero-patchy particles with four precisely located and individual patches (**Figure *2***b-m). Notably, we detected several particles with the outlined particle shape. The patches introduced with the flat stamp revealed a less narrow patch distribution as outlined in Figure S12. The method is capable of, but not restricted to, introducing orthogonal fluorescent materials to the different patch areas. As the method is applicable also to other, more functional materials, we anticipate a high potential in the field of anisotropic particles.

Conclusion

We introduce a robust method designed to add multiple, precisely localized enthalpic patches to monodisperse silicon dioxide (SiO_2) microspheres at equatorial positions, yielding particles with a C_{4v} and C_{2v} symmetry with a high local and chemical precision. For functionalization, we developed a modified microcontact printing (µCP) technique, involving a polydimethylsiloxane (PDMS) elastomeric stamp with a regularly grooved surface possessing microscale channels, whose dimensions (~4 µm) match the particles' geometry. By employing a solid-phase µCP method, we showed that we can transfer highly functional trialkoxysilanes from the elastomer stamp to the particle's contact faces to enable easy chemical modification and functionalization. With this method, we were able to introduce up to four distinct patches possessing orthogonal material properties. Being adaptable to other particle dimensions and surface chemistries, we anticipate a significant potential of the method for the fabrication of various kinds of anisotropically functionalized particles.

Acknowledgement

The authors gratefully acknowledge the financial support of European Research Council (ERC) in the framework of the project REPLICOLL (Grant No. 648365). The authors thank the NMR core facility of the Institute of Chemistry (University of Potsdam). M.R. and R. G. acknowledge the German Research Foundation (DFG) for financial support (project number 471323994). M. H. gratefully acknowledges funding by the Emmy-Noether-Program of the German Research Foundation (Deutsche Forschungsgemeinschaft, DFG; HA 7725/2-1, project number 445804074). The authors acknowledge the company ZUMOLab GmbH (Wesseling, Germany), which manufactured the printing device "ZUMO-MCP (Micro Contact Printer)" that is used in this study.

References:

[1] Z. Zhang, S. C. Glotzer, *Nano Lett.* **2004**, *4*, 1407.
[2] F. Sciortino, E. Bianchi, J. F. Douglas, P. Tartaglia, *J. Chem. Phys.* **2007**, *126*, 194903.
[3] A. B. Pawar, I. Kretzschmar, *Macromol. Rapid Commun.* **2010**, *31*, 150.
[4] S. Ravaine, E. Duguet, *Curr. Opin. Colloid Interface Sci.* **2017**, *30*, 45.
[5] G.-R. Yi, D. J. Pine, S. Sacanna, *J. Phys. Condens. Matter* **2013**, *25*, 193101.
[6] W. Li, H. Palis, R. Mérindol, J. Majimel, S. Ravaine, E. Duguet, *Chem. Soc. Rev.* **2020**, *49*, 1955.
[7] D. Morphew, J. Shaw, C. Avins, D. Chakrabarti, *ACS Nano* **2018**, *12*, 2355.
[8] D. Chen, G. Zhang, S. Torquato, *J. Phys. Chem. B* **2018**, *122*, 8462.
[9] Z.-W. Li, Y.-W. Sun, Y.-H. Wang, Y.-L. Zhu, Z.-Y. Lu, Z.-Y. Sun, *Nanoscale* **2020**, *12*, 4544.
[10] X. Zheng, M. Liu, M. He, D. J. Pine, M. Weck, *Angew. Chem. Int. Ed.* **2017**, *56*, 5507.
[11] A. Perro, E. Duguet, O. Lambert, J.-C. Taveau, E. Bourgeat-Lami, S. Ravaine, *Angew. Chem. Int. Ed.* **2009**, *48*, 361.
[12] G. Russo, M. Lattuada, *Coll. Surf. A: Physicochem. Eng. Asp.* **2024**, *685*, 133293.
[13] J.-G. Park, J. D. Forster, E. R. Dufresne, *Langmuir* **2009**, *25*, 8903.
[14] A. Désert, I. Chaduc, S. Fouilloux, J.-C. Taveau, O. Lambert, M. Lansalot, E. Bourgeat-Lami, A. Thill, O. Spalla, S. Ravaine, E. Duguet, *Polym. Chem.* **2012**, *3*, 1130.
[15] M. Liu, F. Dong, N. S. Jackson, M. D. Ward, M. Weck, *J. Am. Chem. Soc.* **2020**, *142*, 16528.
[16] A. H. Gröschel, A. Walther, T. I. Löbling, F. H. Schacher, H. Schmalz, A. H. E. Müller, *Nature* **2013**, *503*, 247.
[17] F. Tu, D. Lee, *J. Am. Chem. Soc.* **2014**, *136*, 9999.
[18] Z. Gong, T. Hueckel, G.-R. Yi, S. Sacanna, *Nature* **2017**, *550*, 234.
[19] S. Zhai, H. Sun, B. Qiu, H. Zou, *Mater. Adv.* **2020**, *1*, 197.
[20] C. Kaewsaneha, P. Tangboriboonrat, D. Polpanich, M. Eissa, A. Elaissari, *Colloids Surf. A: Physicochem. Eng. Asp.* **2013**, *439*, 35.
[21] A. Walther, A. H. E. Müller, *Chem. Rev.* **2013**, *113*, 5194.
[22] M. Lattuada, T. A. Hatton, *Nano Today* **2011**, *6*, 286.
[23] Z. He, I. Kretzschmar, *Langmuir* **2012**, *28*, 9915.
[24] A. B. Pawar, I. Kretzschmar, *Langmuir* **2009**, *25*, 9057.
[25] Z. He, I. Kretzschmar, *Langmuir* **2013**, *29*, 15755.
[26] S. Lamping, C. Buten, B. J. Ravoo, *Acc. Chem. Res.* **2019**, *52*, 1336.

[27] T. Kaufmann, B. J. Ravoo, *Polymer Chem.* **2010**, *1*, 371.
[28] D. John, M. Zimmermann, A. Böker, *Soft Matter* **2018**, *14*, 3057.
[29] M. Zimmermann, D. John, D. Grigoriev, N. Puretskiy, A. Böker, *Soft Matter* **2018**, *14*, 2301.
[30] F. N. Mehr, D. Grigoriev, N. Puretskiy, A. Böker, *Soft Matter* **2019**, *15*, 2430.
[31] F. Naderi Mehr, D. Grigoriev, R. Heaton, J. Baptiste, A. J. Stace, N. Puretskiy, E. Besley, A. Böker, *Small* **2020**, *16*, 2000442.
[32] P. Akarsu, R. Grobe, J. Nowaczyk, M. Hartlieb, S. Reinicke, A. Böker, M. Sperling, M. Reifarth, *ACS Appl. Polym. Mater.* **2021**, *3*, 2420.
[33] N. Pallab, S. Reinicke, J. Gurke, R. Rihm, S. Kogikoski, M. Hartlieb, M. Reifarth, *Polym. Chem.* **2024**, *15*, 853.
[34] P. Akarsu, S. Reinicke, A.-C. Lehnen, M. Bekir, A. Böker, M. Hartlieb, M. Reifarth, *Small* **2023**, *19*, 2301761.
[35] A. Gharibi, H. Eslami, F. Müller-Plathe, *J. Chem. Theory Comput.* **2024**, DOI 10.1021/acs.jctc.4c00540.
[36] P. Chassagne, P. Garrigue, A. Kuhn, *Adv. Mater.* **2024**, *36*, 2307539.
[37] L. Wang, U. S. Schubert, S. Hoeppener, *Chem. Soc. Rev.* **2021**, *50*, 6507.
[38] M. Sperling, M. Reifarth, R. Grobe, A. Böker, *Chem. Commun.* **2019**, *55*, 10104.
[39] S. Kim, H.-D. Choi, I.-D. Kim, J.-C. Lee, B. K. Rhee, J. A. Lim, J.-M. Hong, *J. Colloid Interface Sci.* **2012**, *368*, 9.